

Complex Motion and Interactive Pattern Formation of Active Brownian Particles

Frank Schweitzer

Institute of Physics, Humboldt University Berlin
GMD Institute for Autonomous Intelligent Systems - AIS, St. Augustin
e-mail: schweitzer@gmd.de
<http://sunma.physik.hu-berlin.de/~frank/>

in Collaboration with:

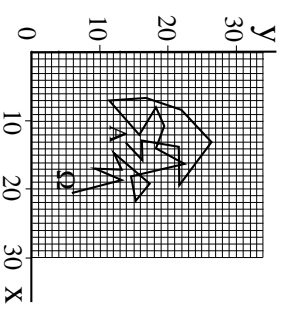
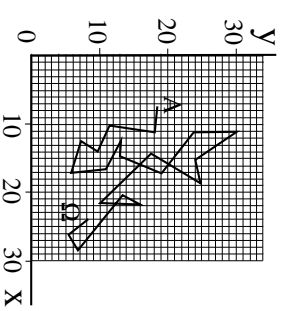
Werner Ebeling (Berlin)
Lutz Schimansky-Geyer (Berlin)
Benno Tlich (Stuttgart)

Schedule of this talk:

1. Concept of Active Brownian Particles
2. Brownian Particles with Internal Energy Depot
3. Interacting Brownian Particles
4. Conclusions

Slide 1

Observation of Brownian Motion



The position of the Brownian particle (radius $0.4 \mu\text{m}$) is documented on a millimeter grid in time intervals $t_0 = 30$ seconds.

Slide 2

Equations for Brownian Particles

- stochastic approach \Rightarrow Langevin equation:

$$\frac{d\mathbf{r}_i}{dt} = \mathbf{v}_i \quad ; \quad m \frac{d\mathbf{v}_i}{dt} = -\gamma_0 \mathbf{v}_i + \mathcal{F}^{stoch}$$

γ_0 : friction coefficient of motion

\mathcal{F}^{stoch} : stochastic force

$$\langle \mathcal{F}^{stoch}(t) \rangle = 0 \quad ; \quad \langle \mathcal{F}^{stoch}(t) \mathcal{F}^{stoch}(t') \rangle = 2S \delta(t - t')$$

fluctuation-dissipation theorem: $S = k_B T \gamma_0$

- overdamped limit: $d\mathbf{v}_i/dt = 0$, or $\gamma_0 \rightarrow \infty$

$$\frac{d\mathbf{r}_i}{dt} = \sqrt{2D_n} \boldsymbol{\xi}(t) \quad ; \quad D_n = \frac{k_B T}{\gamma_0} = \frac{\varepsilon}{\gamma_0}$$

D_n : spatial diffusion coefficient of the particles

$\boldsymbol{\xi}(t)$: white noise, $\langle \boldsymbol{\xi}_i(t) \boldsymbol{\xi}_j(t') \rangle = \delta_{ij} \delta(t - t')$.

Active Brownian Particles

“Active Brownian particles are Brownian particles with internal degrees of freedom. They have the ability to take up energy from the environment, to store it in an internal depot and to convert internal energy to perform different activities, such as metabolism, motion, change of the environment, or signal-response behavior.”

internal degrees of freedom:

1. internal energy depot: $e_i(t)$
 - take-up, storage, conversion of internal energy
 - \rightarrow pumped Brownian particles, Brownian motions
2. discrete internal states: $\theta_i(t)$
 - generation of different components of a self-consistent field
 - sensitivity to different field components
 - \rightarrow *non-linear feedback* \Rightarrow *interactive structure formation* on the macroscopic level

advantages:

- particle-based approach to structure formation
- complete stochastic dynamics, based on Langevin equations
- consideration of energetic aspects
- interaction between particles via multicomponent field
- external eigendynamics of the field

Brownian Particle with Internal Energy Depot

Depot $e(t) \Rightarrow$ internal storage of energy

$$\frac{d}{dt}e(t) = q(\mathbf{r}) - c e(t) - d(\mathbf{v}) e(t)$$

$q(\mathbf{r})$: gain \Rightarrow space-dependent take-up of energy

c : loss \Rightarrow internal dissipation

$d(\mathbf{v})$: conversion of internal into kinetic energy

simple ansatz: $d(\mathbf{v}) = d_2 v^2$; $d_2 > 0$

Total energy $E(t)$ and mechanical energy $E_0(t)$:

$$E(t) = E_0(t) + e(t) \quad E_0(t) = \frac{m}{2} v^2 + U(\mathbf{r})$$

balance equation: $\frac{d}{dt}E_0(t) = (d_2 c(t) - \gamma_0) v^2$

$$\Rightarrow \quad m r \ddot{\mathbf{r}} + \dot{\mathbf{r}} \nabla U(\mathbf{r}) = (d_2 c(t) - \gamma_0) \mathbf{r}^2$$

Stochastic equation for Brownian particles with energy depot

$$m \dot{\mathbf{v}} + \gamma_0 \mathbf{v} + \nabla U(\mathbf{r}) = d_2 e(t) \mathbf{v} + \mathcal{F}(t)$$

Balance equation for the stochastic case with $S = k_B T$ γ_0 :

$$\frac{d}{dt} \left(\frac{1}{2} m v^2 + U(\mathbf{r}) \right) = d_2 e(t) v^2$$

Slide 5

Non-linear Friction Function

equations of motion:

$$\dot{\mathbf{v}} + \gamma_0 \mathbf{v} + \nabla U(\mathbf{r}) = d_2 e(t) \mathbf{v} + \mathcal{F}(t)$$

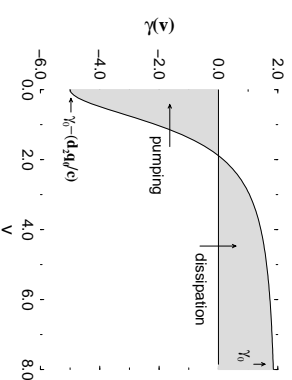
$$\frac{d}{dt}e(t) = q(\mathbf{r}) - c e(t) - d(\mathbf{v}) e(t)$$

$$\Rightarrow \quad \gamma(\mathbf{v}) = \gamma_0 - d_2 e(t)$$

assumptions: $q(\mathbf{r}) \equiv q_0$; $d(\mathbf{v}) = d_2 v^2$; $\dot{e}(t) = 0$

$$e_0 = \frac{q_0}{c + d_2 v^2}$$

$$\Rightarrow \quad \gamma(\mathbf{v}) = \gamma_0 - \frac{q_0 d_2}{c + d_2 v^2} \quad \text{zero: } v_0^2 = \frac{q_0}{d_2} - \frac{c}{d_2}$$



Slide 6

Fokker-Planck Equation

distribution function: $p(\mathbf{r}, \mathbf{v}, e, t)$

$$\frac{\partial p(\mathbf{r}, \mathbf{v}, e, t)}{\partial t} = \frac{\partial}{\partial \mathbf{v}} \left\{ \gamma_0 - \frac{d_2 e}{m} \mathbf{v} p(\mathbf{r}, \mathbf{v}, e, t) + D \frac{\partial p(\mathbf{r}, \mathbf{v}, e, t)}{\partial \mathbf{v}} \right\} - \mathbf{v} \frac{\partial p(\mathbf{r}, \mathbf{v}, e, t)}{\partial \mathbf{r}} + \frac{1}{m} \nabla U(\mathbf{r}) \frac{\partial p(\mathbf{r}, \mathbf{v}, e, t)}{\partial \mathbf{v}} - \frac{\partial}{\partial e} [q(\mathbf{r}) - c e - d_3 v^2 e] p(\mathbf{r}, \mathbf{v}, e, t)$$

Fokker-Planck equation for $p(\mathbf{v}, t)$ with $e(t) \rightarrow e_0 = \frac{\gamma_0}{c + d_3 v^2}$

$$\frac{\partial p(\mathbf{v}, t)}{\partial t} = \frac{\partial}{\partial \mathbf{v}} \left[\left(\gamma_0 - \frac{d_2 e_0}{c + d_2 v^2} \right) \mathbf{v} p(\mathbf{v}, t) + D \frac{\partial p(\mathbf{v})}{\partial \mathbf{v}} \right]$$

stationary solution: $p^0(\mathbf{v}, t) = 0$

$$p^0(\mathbf{v}) = C' (c + d_2 v^2)^{\gamma_0/2D} \exp \left\{ -\frac{\gamma_0}{2D} v^2 \right\}$$

normalization: $\int d\mathbf{v} p^0(\mathbf{v}) = 1 \Rightarrow C'$

Slide 7

Stationary Velocity Distribution

small v^2 : power series

$$p^0(\mathbf{v}) \sim \exp \left\{ -\frac{\gamma_0}{2D} \left(1 - \frac{q_0 d_2}{c \gamma_0} \right) v^2 + \dots \right\}$$

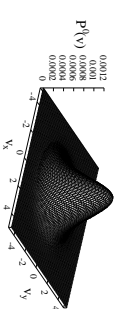
two-dimensional space: $\mathbf{v} = v_x + v_y$

$q_0 d_2 < c \gamma_0$: subcritical pumping

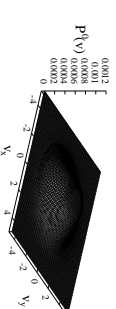
\Rightarrow Maxwellian velocity distribution

$q_0 d_2 > c \gamma_0$: supercritical pumping

\Rightarrow crater-like distribution



$d_2 = 0.07$



$d_2 = 0.2$



$d_2 = 0.7$

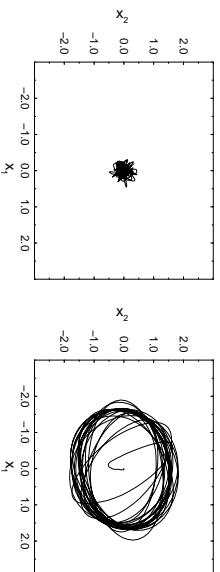
Normalized stationary solution $p^0(\mathbf{v})$, $\gamma_0 = 2$, $D = 2$, $c = 1$, $q_0 = 10$.

Slide 8

Critical Supply of Energy

assumption: motion in two dimensions

$$q(x_1, x_2) = q_0 \quad U(x_1, x_2) = \frac{d}{2}(x_1^2 + x_2^2)$$



$q_0 = 0.0$: simple Brownian motion;
 $q_0 = 1.0$: motion on a stochastic limit cycle

Brownian particle as micro-motor:

- efficiency ratio:

$$\sigma = \frac{dE_{out}/dt}{dE_{in}/dt} = \frac{d_2 e v^2}{q_0}$$

- energy depot in quasi-stationary equilibrium: $e = \frac{q_0}{c + d_2 v^2}$
- v approximated by the stationary velocity:

$$v_0^2 = (v_1^2 + v_2^2) = \frac{q_0}{\gamma_0} - \frac{c}{d_2}$$

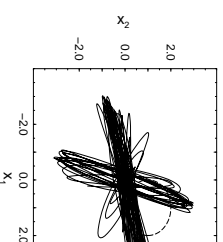
$$\Rightarrow \sigma = 1 - \frac{c \gamma_0}{d_2 q_0} \quad \sigma > 0 \quad \text{only if} \quad q_0 > q_0^{crit} = \frac{\gamma_0 c}{d_2}$$

Slide 9

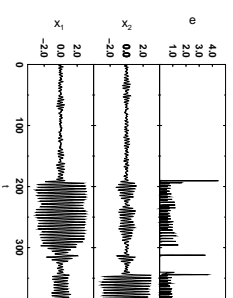
Localized Energy Sources

- parabolic potential: $U(x_1, x_2) = \frac{d}{2}(x_1^2 + x_2^2)$
- take-up of energy in a restricted area:

$$q(x_1, x_2) = \begin{cases} q_0 & \text{if } [(x_1 - b_1)^2 + (x_2 - b_2)^2] \leq R^2 \\ 0 & \text{else} \end{cases}$$



- motion into the energy area becomes accelerated
- \Rightarrow oscillatory movement with fixed direction



- intermittent type of motion
- new cycles start with a burst of energy
- increase in d_2 abridges the cycle \Rightarrow directed motion more susceptible to become Brownian motion

Slide 10

Passive and Active Modes of Motion

one-dimensional case, $m = 1$, $q(\mathbf{r}) = q_0$, $\mathbf{F} = -\nabla U$

$$\dot{\mathbf{x}} = \mathbf{v}$$

$$\dot{v} = -(\gamma_0 - d_2 e(t))\mathbf{v} + \mathbf{F} + \sqrt{2D}\boldsymbol{\xi}(t)$$

$$\dot{e} = q_0 - ce - d_2 v^2 e$$

stationary solutions: ($D = 0$)

$$\mathbf{v}_0 = \frac{\mathbf{F}}{\gamma_0 - d_2 e_0} \quad ; \quad e_0 = \frac{q_0}{c + d_2 \mathbf{v}_0^2}$$

$$\Rightarrow \left[d_2 \gamma_0 \mathbf{v}_0^2 - d_2 \mathbf{F} v_0 - (q_0 d_2 - c \gamma_0) \right] v_0 = c \mathbf{F}$$

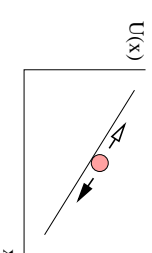
- always existing: $\mathbf{v}_0(\mathbf{x}) \sim \mathbf{F}(\mathbf{x})$
 \Rightarrow analytic continuation of Stokes' law: $\mathbf{v}_0 = \mathbf{F}/\gamma_0$
- subcritical supply of energy:
 \Rightarrow *passive* motion driven by \mathbf{F}
- supercritical supply of energy: 3 solutions
 \Rightarrow "high velocity" or *active* mode of motion
 \Rightarrow motion *in* or *against* the direction of \mathbf{F}

Slide 11

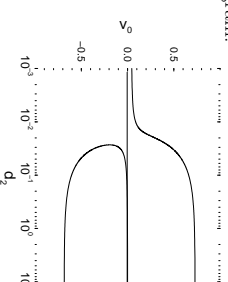
Solutions for $\mathbf{F} = \text{const.} \neq 0$

stationary solutions:

$$d_2 \gamma_0 \mathbf{v}_0^3 - d_2 \mathbf{F} v_0^2 - (q_0 d_2 - c \gamma_0) v_0 - c \mathbf{F} = 0$$



bifurcation diagram:



stability analysis \Rightarrow *stable* uphill motion ($c \rightarrow 0$):

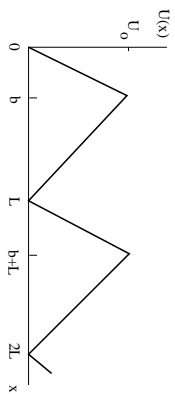
$$d_2^{crit} = \frac{F^4}{8q_0^2} \left(1 + \sqrt{1 + \frac{4\gamma_0 q_0}{F^2}} \right)^3$$

Slide 12

Motion in a Ratchet Potential

one-dimensional motion, $q(x) = q_0$, periodic potential:

$$U(x) = \begin{cases} U_0 \{x - nL\} & \text{if } nL \leq x \leq nL + b \\ \frac{U_0}{L-b} \{(n+1)L - x\} & \text{if } nL + b \leq x \leq (n+1)L \end{cases}$$



equations of motion:

$$\dot{\mathbf{x}} = \mathbf{v}$$

$$\dot{\mathbf{v}} = -[\gamma_0 - d_2 e(t)] \mathbf{v} - \frac{\partial U(x)}{\partial x} + \sqrt{2k_B T \gamma_0} \boldsymbol{\xi}(t)$$

$$\dot{e} = q_0 - ce - d_2 v^2 e$$

overdamped limit:

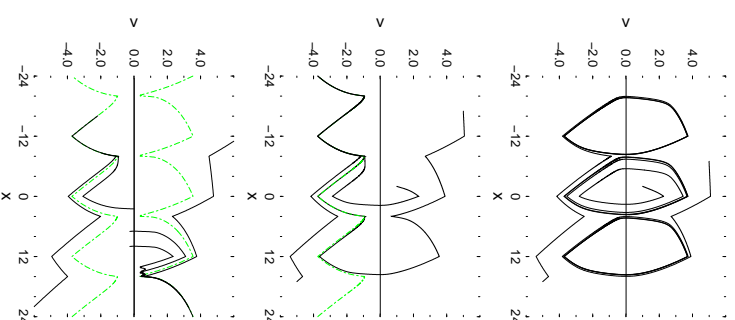
$$\mathbf{v}(t) = -\frac{1}{\gamma_0 - d_2 e(t)} \frac{\partial U}{\partial \mathbf{x}} + \frac{\sqrt{2k_B T \gamma_0}}{\gamma_0 - d_2 e(t)} \boldsymbol{\xi}(t)$$

with $e(t) \rightarrow e_0 = \frac{q_0}{c + d_2 v^2}$:

$$f(t) = \frac{1}{\gamma_0 - d_2 e(t)} \Rightarrow f(x) = \frac{1}{2\gamma_0 F_1} (F_1 \pm \sqrt{F_1^2 + 4q_0 \gamma_0})$$

$$f_1(x) > 0, f_2(x) < 0; (\gamma_0 - d_2 e_0) \tau = 0$$

Slide 13

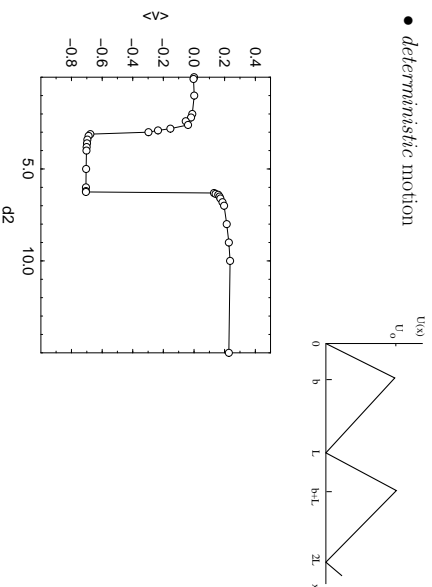


Phase-space trajectories of particles starting with different initial conditions, for three different values of the conversion parameter d_2 : (top) $d_2 = 1$, (middle) $d_2 = 4$, (bottom) $d_2 = 14$. The dashed-dotted lines show the attractor of the delocalized motion which is obtained in the long-time limit.

Slide 14

Net Current Dependence on d_2

- 10,000 particles with random initial positions in $\{0, L\}$
- *deterministic* motion

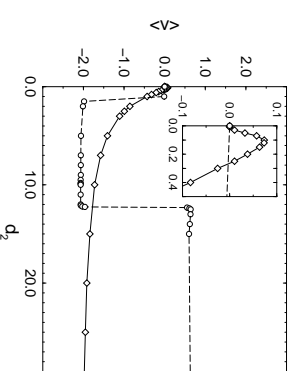


- $d_2 < d_2^{crit1}$ no net current
 - $d_2^{crit1} < d_2 < d_2^{crit2}$ negative net current
 - $d_2^{crit2} < d_2$ positive net current
- $$d_2^{crit1} = \frac{F^4}{8q_0^3} \left(1 + \sqrt{1 + \frac{4\gamma_0 q_0}{F^2}} \right)^3$$

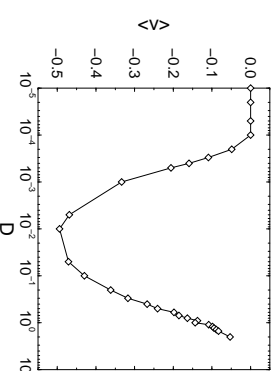
Slide 15

Net Current Dependence on d_2 and D

- 10,000 particles; less damped case, random initial conditions
- deterministic case: $D = 0$: \circ , stochastic case: $D = 0.01$: \diamond

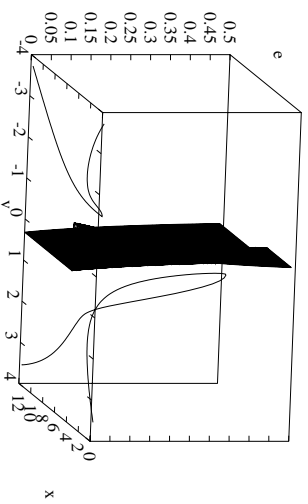


- fixed conversion parameter: $d_2 = 1.0$
- ⇒ Existence of *critical* and *optimal* D



Slide 16

Separatrix and Asymptotic Trajectories



Active Brownian Particles Responding to a Field

active particles:

- characterized by an internal degree of freedom: $\theta_i(t)$, which can be changed: $w(\theta_i|\theta)$

- Langevin equation:

$$\frac{d\mathbf{r}_i}{dt} = \mathbf{v}_i; \quad \frac{d\mathbf{v}_i}{dt} = -\gamma\mathbf{v}_i + \alpha_i \frac{\partial h^\varepsilon(\mathbf{r}, t)}{\partial \mathbf{r}} \Big|_{\mathbf{r}_i} + \sqrt{2\varepsilon_i\gamma} \boldsymbol{\xi}_i(t)$$

overdamped limit:

$$\frac{d\mathbf{r}_i}{dt} = \frac{\alpha_i}{\gamma} \frac{\partial h^\varepsilon(\mathbf{r}, t)}{\partial \mathbf{r}} \Big|_{\mathbf{r}_i} + \sqrt{\frac{2\varepsilon_i}{\gamma}} \boldsymbol{\xi}_i(t)$$

$h^\varepsilon(\mathbf{r}, t)$: effective field

- “individual” parameters (may depend on θ_j):

α_i : individual response to the field

– attraction: $\alpha_i > 0$, or repulsion: $\alpha_i < 0$

– threshold h_0 : $\alpha_i = \Theta[h^\varepsilon(\mathbf{r}, t) - h_0]$, $\Theta[y] = 1$, if $y > 0$

– internal value θ : $\alpha_i = \delta(\theta_i - \theta)$

ε_i : individual intensity of noise

– measure of the *sensitivity* s_i of the particle: $s_i \propto 1/\varepsilon_i$.

Slide 18

Effective Field

- Langevin eq.: particles respond to the gradient of $h^\varepsilon(\mathbf{r}, t)$
- effective field: a specific function of the different field components $h_\theta(\mathbf{r}, t)$:

$$\nabla h^\varepsilon(\mathbf{r}, t) = \nabla h^\varepsilon(\dots, h_\theta(\mathbf{r}, t), h_\theta(\mathbf{r}, t), \dots)$$

- particles with internal parameter θ generate a field $h_\theta(\mathbf{r}, t)$ which obeys a reaction-diffusion equation:

$$\frac{dh_\theta(\mathbf{r}, t)}{dt} = -k_\theta h_\theta(\mathbf{r}, t) + D_\theta \Delta h_\theta(\mathbf{r}, t) + \sum_{i=1}^N q_i(\theta_i, t) \delta(\theta - \theta_i(t)) \delta(\mathbf{r} - \mathbf{r}_i(t))$$

spatio-temporal evolution of the field, $h_\theta(\mathbf{r}, t)$:

- decay with rate k_θ
- diffusion (coefficient D_θ)
- production with individual rate $q_i(\theta_i, t)$

Slide 19

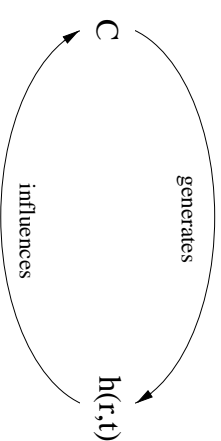
Complete Dynamics for N Active Particles

- N active Brownian particles:
internal parameters $\theta_1, \dots, \theta_N$; positions $\mathbf{r}_1, \dots, \mathbf{r}_N$
canonical N -particle distribution function:
 $P(\underline{\mathbf{r}}, \underline{\theta}, t) = P(\mathbf{r}_1, \theta_1, \dots, \mathbf{r}_N, \theta_N, t)$
- changes:
 - (i) movement: $r_i \rightarrow r_i'$
 - (ii) transition: $\theta_i \rightarrow \theta_i'$ with probability $w(\theta_i'|\theta_i)$
- multivariate master equation:
limit of strong damping: $\gamma_0 \rightarrow \infty$, and $\alpha_i = \alpha$, $\epsilon_i = \epsilon$:
$$\frac{\partial}{\partial t} P(\underline{\mathbf{r}}, \underline{\theta}, t) = - \sum_{i=1}^N \{ \nabla_i ((\alpha/\gamma_0) \nabla_i h^c(\mathbf{r}, t) P(\underline{\mathbf{r}}, \underline{\mathbf{r}}, t)) - D_n \Delta_i P(\underline{\mathbf{r}}, \underline{\theta}, t) \}$$

$$+ \sum_{i=1}^N \sum_{\theta_i' \neq \theta_i} \{ w(\theta_i'|\theta_i) P(\theta_i', \underline{\mathbf{r}}, t) - w(\theta_i|\theta_i') P(\theta_i, \underline{\mathbf{r}}, t) \}$$
- dynamics of the effective field $h^c(\mathbf{r}, t)$

Slide 20

Examples of Circular Causation

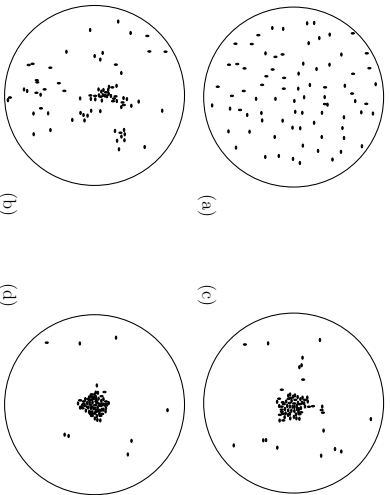


- active particles are identical \Rightarrow no transitions
 $\alpha_i = \alpha > 0$, $\epsilon_i = \epsilon$, $\theta_i = 0$, $q_i(\theta_i, t) = q_0 = \text{const.}$
- one-component field:
$$\nabla_i h^c(\mathbf{r}, t) = \nabla_i h(\mathbf{r}, t)$$

$$\frac{dh(\mathbf{r}, t)}{dt} = -k_0 h(\mathbf{r}, t) + D_0 \Delta h(\mathbf{r}, t) + q_0 \sum_{i=1}^N \delta(\mathbf{r} - \mathbf{r}_i(t))$$
- **applications:**
 - biological aggregation:
cells; slime mold amoebae; myxobacteria generate a *chemical field* to communicate
 - track formation:
bacteria; pedestrians mark their track, which can be reinforced by other individuals (usually $D_0 = 0$)

Slide 21

Aggregation of Larvae

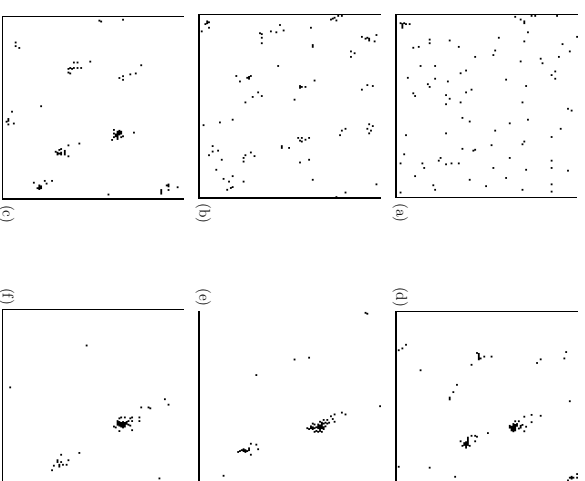


Aggregation of larvae of the bark beetle *Dendroctonus micans*. Total population 80 larvae, density 0.166 larvae/cm². Time in minutes: (a) $t = 0$, (b) $t = 5$, (c) $t = 10$, (d) $t = 20$.

Dorenbout, J. L.; Gregoire, J. C.; Le Fort, E.: Kinetics of Larval Gregarious Behavior in the Bark Beetle *Dendroctonus micans* (Coleoptera: Scolytidae). *J. Insect Behavior* **3/2**, 169-182 (1990)

Slide 22

Aggregation of Active Brownian Particles

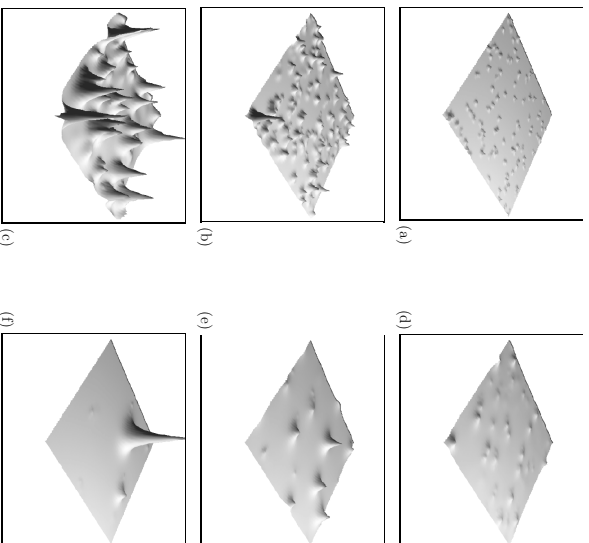


Position of 100 active Brownian particles moving on a triangular lattice (size: $A = 100 \times 100$). Time in simulation steps: (a) $t = 100$, (b) $t = 1,000$, (c) $t = 5,000$, (d) $t = 10,000$, (e) $t = 25,000$, (f) $t = 50,000$.

Schweitzer, F.; Schimansky-Gier, L.: Clustering of Active Walkers in a Two-Component System. *Physica A* **206**, (1994) 356-379

Slide 23

Evolution of the Self-Consistent Field

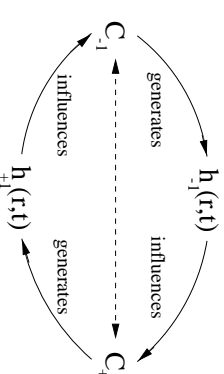


Time in simulation steps. (left side) Growth regime: (a) $t = 10$, (b) $t = 100$, (c) $t = 1,000$. (right side) Competition regime: (d) $t = 1,000$, (e) $t = 5,000$, (f) $t = 50,000$. The scale of the right side is 10 times the scale of the left side. Hence, Fig. (d) is the same as Fig. (c).

Schweitzer, F.: Schimansky-Gajer, L.: Clustering of Active Walkers in a Two-Component System, *Physica A* 206, (1994) 359-379

Slide 24

Examples of Circular Causation



- active particles with two different states $\theta \in \{-1, +1\}$, transitions possible
- state dependent production rate
- two-component field

$$q_i(\theta_i, t) = \frac{\theta_i}{2} [(1 + \theta_i) q_i(+1, t) - (1 - \theta_i) q_i(-1, t) - 1]$$

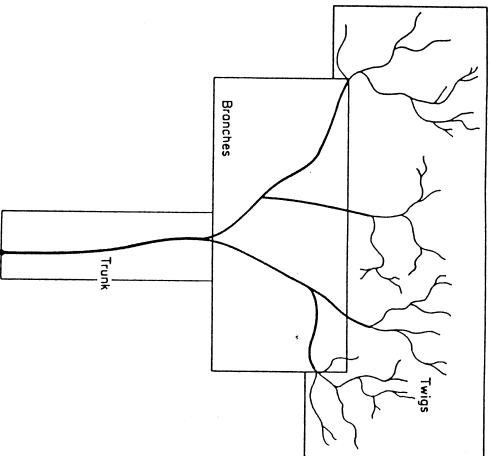
$$\frac{dh_\theta(\mathbf{r}, t)}{dt} = -k_\theta h_\theta(\mathbf{r}, t) + \sum_{i=-1}^N q_i(\theta_i, t) \delta(\theta - \theta_i(t)) \delta(\mathbf{r} - \mathbf{r}_i(t))$$

applications:

- exploitation of food sources: ants mark trails from food sources to the nest with additional chemicals to guide nestmates to resources
- self-assembling of networks: particles responding to two different fields, link nodes with opposite potential

Slide 25

Foraging Route of Ants (*Pheidole mitchellii*)

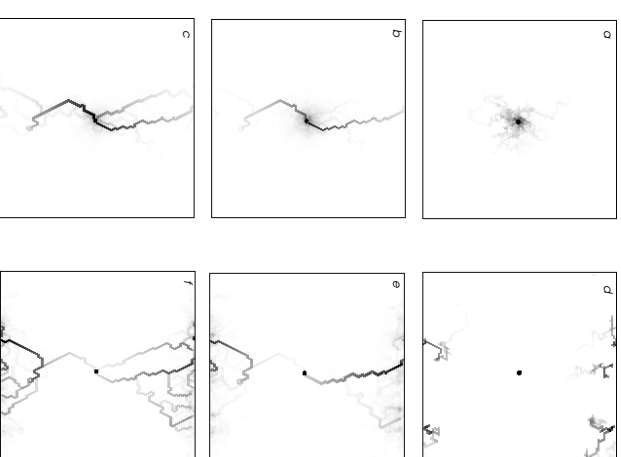


Schematic representation of the complete foraging route of *Pheidole mitchellii*, a harvesting ant of the southwestern U.S. deserts. Each day tens of thousands of workers move out to the dendritic trail system, disperse singly, and forage for food.

Hölldobler, B. and Mehlhah, M.: The foraging system of *Pheidole mitchellii* (Hymenoptera: Formicidae), *Insectes Sociaux* **27/3** (1980) 237-264

Slide 26

Trunk Trail Formation to Extended Forage Areas

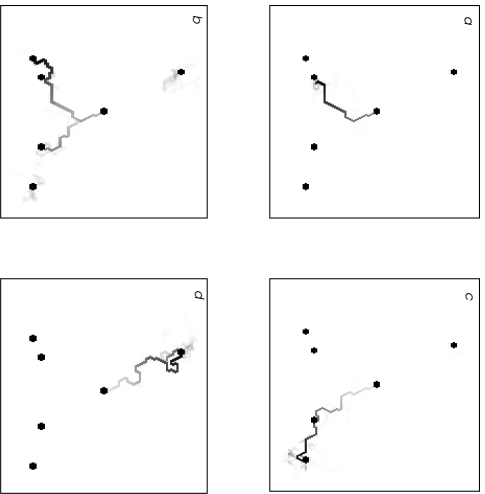


Formation of trails from a nest (middle) to a line of food at the top and the bottom of a lattice. (a-c) show the distribution of chemical component (+1), and (d-f) show the distribution of chemical component (-1). Time in simulation steps: (a), (d) $t = 1,000$, (b), (e) $t = 5,000$, (c), (f) $t = 10,000$.

Schweitzer, F., Luo, K., Faganly, F.: Active Random Walkers Simulate Trunk Trail Formation by Ants, *BioSystems* **41** (1997) 153-166

Slide 27

Trunk Trail Formation to Separate Food Items

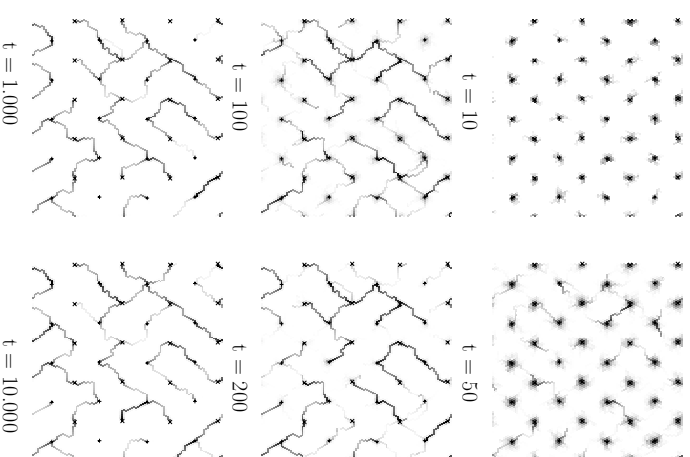


Formation of trails from a nest (middle) to five randomly placed food clusters. The distribution of chemical component (-1) is shown after (a) 2000, (b) 4000, (c) 8500, and (d) 15000 simulation time steps, respectively.

Schweitzer, F.; Lao, K.; Family, F.: Active Random Walkers Simulate Trunk Trail Formation by Ants, *Biosystems* 41 (1997) 153-166

Slide 28

Formation of Networks



Time series of the evolution of a network (time in simulation steps). Lattice size 100×100 , 5000 particles, 40 nodes, $z_+ = 20$, $z_- = 20$. Parameters: $\phi_0 = 10,000$, $k_0 = 0.03$, $\beta = 0.2$.

Slide 29

Conclusions

1. Model of Active Brownian Particles:

- particle-based model for interactive structure formation
- relation to biology:
- (a) energy consumption for metabolism and motion
- (b) interaction with the environment due to a self-consistent multicomponent field \Rightarrow non-linear feedback

2. Conversion of Brownian Motion into Directed Motion:

- (a) quasiperiodic movement of the particles between energy sources and "home"
- (b) directed movement in a asymmetric periodic potential \Rightarrow direction depends on conversion parameter d_2 and noise D
- (c) chemotactic response to a self-consistent chemical field two-component field \Rightarrow directed forward / backward motion

3. Advantage of the Active Brownian Particles Model:

- stochastic approach to directed movement and structure formation
- efficient and stable simulation algorithm: instead of integrating PDE \Rightarrow simulation of the Langevin equation
- applicable to systems where only small particle numbers govern the system dynamics

References

- [1] Ebeling, W., Erdmann, U., Schimansky-Geier, L., Schweitzer, F. (1999). Brownian Particles far from Equilibrium, *European Journal of Physics B* (to be submitted).
- [2] Ebeling, W.; Schweitzer, F.; Tllich, B. (1999). Active Brownian Particles with Energy Depots Modelling Animal Mobility. *BioSystems* **49**, 17-29.
- [3] Helbing, D.; Schweitzer, F.; Keltsch, J.; Molnar, P. (1997). Active Walker Model for the Formation of Human and Animal Trail Systems, *Physical Review E* **56/3**, 2527-2539.
- [4] Schimansky-Geier, L.; Schweitzer, F.; Mieth, M. (1997). Interactive Structure Formation with Brownian Particles, in: F. Schweitzer (ed.): *Self-Organization of Complex Structures: From Individual to Collective Dynamics*, London: Gordon and Breach, pp. 101-118.
- [5] Schweitzer, F. (1997). Active Brownian Particles: Artificial Agents in Physics, in: L. Schimansky-Geier, T. Pöschel (eds.): *Stochastic Dynamics* (Lecture Notes in Physics vol. 484), Berlin: Springer, pp. 358-371.
- [6] Schweitzer, F.; Ebeling, W.; Tllich, B. (1998). Complex Motion of Brownian Particles with Energy Depots, *Physical Review Letters* **80/23**, 5044-5047.
- [7] Schweitzer, F.; Tllich, B.; Ebeling, W. (1999). High Velocity Mode for Brownian Particles in a Ratchet Potential, *Physical Review E* (submitted).
- [8] Schweitzer, F.; Lao, K.; Family, F. (1997). Active Random Walkers Simulate Trunk Trail Formation by Ants, *BioSystems* **41**, 153-166.
- [9] Schweitzer, F.; Schimansky-Geier, L. (1994). Clustering of Active Walkers in a Two-Component System, *Physica A* **206**, 359-379.
- [10] Stevens, A.; Schweitzer, F. (1997). Aggregation Induced by Diffusing and Non-diffusing Media, in: W. Alt, A. Deutsch, G. Dunn (eds.): *Dynamics of Cell and Tissue Motion*, Basel: Birkhäuser, pp. 183-192.
- [11] Tllich, B., Schweitzer, F., Ebeling, W. (1999). Directed Motion of Brownian Particles with Internal Energy Depot, *Physica A* (in press).